Cu-(U) mineralisation in the copper sandstones at Šafárka occurrence near Novoveská Huta (Spišská Nová Ves), Spišsko-gemerské Rudohorie Mts., Western Carpathians, Gemeric Unit, eastern Slovakia

Štefan Ferenc[1*], Tomáš Mikuš[2], Richard Kopáčik[1], Jozef Vlasáč[2] & Eva Hoppanová[1]

[1] Department of Geography and Geology, Faculty of Natural Sciences, Matej Bel University, Tajovského 40, 974 01 Banská Bystrica, Slovakia; stefan.ferenc@umb.sk, richard.kopacik@umb.sk, eva.hoppanova@umb.sk
[2] Earth Science Institute of the Slovak Academy of Sciences, Ďumbierska 1, 974 11 Banská Bystrica, Slovakia; mikus@savbb.sk, vlasac@savbb.sk
*corresponding author

AGEOS

Abstract: Several occurrences of copper sandstone mineralisation type occur in the Permian volcano-sedimentary sequences of the Northern Gemeric Unit (Spišsko-gemerské Rudohorie Mts.). The object of presented mineralogical research was Cu-(U) mineralisation in the copper sandstones at the Šafárka occurrence, located about 4 km SE of Novoveská Huta (part of Spišská Nová Ves district town). Cu-(U) mineralisation was formed in fine-grained psammites of greenish-grey colour. The surface of the samples is limonitised, with coatings of green Cu and U supergene minerals. The main rock-forming mineral is quartz. Carbonate (probably authigenic), muscovite and fragments of sericite shales or highly altered volcanics are present to a lesser extent. Accessories represent K-feldspar, tourmaline and leucoxenised Fe-Ti oxides. Rock matrix is formed mainly by sericite and fine-grained quartz. Ore minerals (chalcopyrite, pyrite – also var. *bravoite*, tennantite-(Fe), uranium-bearing *leucoxene*) form disseminations and veinlets in sandstones. Supergene minerals of Fe, Cu, and U (chalcocite, yarrowite, uranophane-α, goethite, malachite, baryte, anglesite, and cinnabar) fill microscopic cavities and cracks in the rock. Based on the chemical composition, the studied pyrite can be divided into several groups: a) pyrite with a minimum content of admixtures (composition almost corresponding to the formula FeS_2; b) As-bearing pyrite; and c) Ni- and Co-bearing *bravoite*. Arsenic most likely enters the anionic position of pyrite by the substitution $As^{1-} \rightarrow S^{1-}$ and is probably present in solid solution. Zonality of *bravoite* is caused by ranging in Ni content and the corresponding fluctuations in Fe content (negative correlation), at a relatively constant Co content. Studied *bravoite* represents a nice example of the preferred concentration of Ni at the edges of the crystals and growth zones. Formation of uranophane-α documents the neutralisation of the environment during weathering of sandstones. Precipitation of baryte and anglesite caused an increase in the pH of the environment (from acid to the slightly basic), which allowed the precipitation of uranophane-α and malachite.

Keywords: Western Carpathians, Gemeric Unit, Permian, sandstones, copper, uranium, red-ox conditions

1. INTRODUCTION

Infiltration mineralisation of the copper sandstone type is widespread globally and often reaches economic parameters (overview, e. g. Wolf ed., 1976; Evans, 1993; Laznicka, 2006). In the Slovak part of the Carpathians, this type of mineralisation is also present, but the individual sites reach mineralogical parameters or max. deposit occurrence size. The common denominator of these occurrences is their location in the Permian sediments. In the Hronic Unit, U-Cu mineralisation in the Lower Permian Červenec Beds is located on the NE slopes of Nízke Tatry Mts. The most important representative is the deposit occurrence Východná-Nižný Chmelienec (Drnzík, 1969; Rojkovič, 1998). In the Veporic Unit, a similar type of mineralisation was found near Selce in the Starohorské Vrchy Mts. (Rojkovič, 1997; Polák et al., 2015). Copper sandstones also appear near Brezno (Stupka), in the Malé Karpaty Mts. (Smolenice – Lošonec) and in the Považský Inovec Mts. at Kálnica (Rojkovič, 2003). Several occurrences of copper sandstone mineralisation type occur in the Permian volcano-sedimentary sequences of the Northern Gemeric Unit (Stratená, Novoveská Huta, Hnilčík). Copper mineralisation, which was at the end of the 17th century and the beginning of the 18th century also the subject of not very extensive mining, is in the Gemeric Unit locally accompanied by insignificant U mineralisation (Grecula et al., 1995).

The presented contribution is devoted to the mineralogical characteristics of Cu-(U) mineralisation in the copper sandstones at the Šafárka locality (also Trubačovec) near Novoveská Huta (Northern Gemeric Unit).

2. GEOLOGICAL SETTING AND NATURE OF OCCURRENCE

The Gemeric Unit forms a system of north-vergent partial nappes, composed mainly of metamorphic pre-Carboniferous complexes and Upper Palaeozoic to Lower Triassic syn- and post-orogenic formations (Maheľ & Vozár, 1971). It is most often divided into

Manuscript received 2022-02-10
Revised version accepted 2022-08-23

the Northern (Klátov and Rakovec subunits, Črmeľ and Ochtiná subunits) and the Southern (Gelnica Group and Štós Unit) Gemeric units (Fig. 1).

The Gelnica Group is represented as a several thousand meters thick, Lower Palaeozoic volcanogenic (rhyolite-dacite) flysch (Snopko & Ivanička, 1978; Ivanička et al., 1989), whose origin is associated with the active Gondwana margin (Vozárová, 1993; Putiš et al., 2008). The pre-Permian Štós Unit consists of metamorphosed sandstones, phyllites, and rarely metabasalt bodies (Vozárová et al., 2014). Both, sedimentary and volcanic rocks have undergone a regional metamorphosis in the conditions of the chlorite zone of the greenschists facies (Faryad, 1991[a,b]). The Upper Palaeozoic and Triassic sediments of the Gočaltovo and Kobeliarovo groups form the cover sequence of the Southern Gemeric Unit.

The fundament of the Northern Gemeric Unit forms a Lower Palaeozoic (Devonian) Rakovec and Klátov subunits, with oceanic affinity. The Rakovec Subunit consists of low metamorphosed sediments and basic volcanics. The Klátov Subunit (gneisses, amphibolites) represents a fragmented metaophiolite complex (Radvanec et al., 2017) metamorphosed in the amphibolite facies. Both subunits in the current geological structure represent the Variscan ocean suture (Németh, 2002; Radvanec & Németh, 2018). The lower part of the Rakovec Subunit (Middle Devonian) consists of Smrečina Formation (metasandstones, phyllites, spilite-keratophyre volcanics). The Upper Devonian Sykava Formation contains mainly metamorphosed basalts and their volcaniclastics, together with metasandstones and phyllites.

The Late Palaeozoic (Lower Carboniferous) is in the Northern Gemeric Unit represented by the Ochtiná (west) and Črmeľ (east) groups, which are formed by both terrigenous and marine sediments, with carbonate bodies (magnesite), basic volcanics, locally with ultrabasic rocks (Vozárová, 1996). The Upper Carboniferous Dobšiná Group transgress onto a Lower Palaeozoic fundament. Overburden of the basal conglomerates (Rudňany Formation) forms shallow-marine sediments and basic volcanics (Zlatník Formation) and the shallow-water Hámor Formation of terrigenous clastics. The transgressive Krompachy Group (Permian) are lying on the various Northern Gemeric complexes. The Krompachy Group is at the base represented by continental, unsorted coarse clastics (Knola and Petrova Hora formations), which pass to lagoon-sebcha sediments with evaporite deposits (Upper Permian to Lower Triassic of the Novoveská Huta Formation). They are accompanied by subalkaline rhyolite volcanism (Novotný & Mihál', 1987; Hók et al., 2019). The metamorphic conditions of the Carboniferous rocks of the Northern Gemeric Unit range in the lower part of the greenschist facies (low pressures, T ~ 360 °C), on the border of the anchizone and the lower part of greenschist facies, respectively. Metamorphosis of the Permian rocks did not exceed the upper boundary of the anchizone (Vozárová, 1996).

In the Northern Gemeric Unit, copper sandstones within the Permian Krompachy Group appear in two stratigraphic horizons (Fig. 2). The lower, Slivníky horizon is located in the Knola Formation, where copper sandstones form lenticular layers and represent part of the Markušovce sandstones. Cu-(U) mineralisation is found here in the greenish sandstones and surrounding psephites. The copper sandstones of the Slivníky horizon are widespread in the localities of Markušovská dolina, Slivníky, Kráľovský prameň, Žompy and in the studied Šafárka

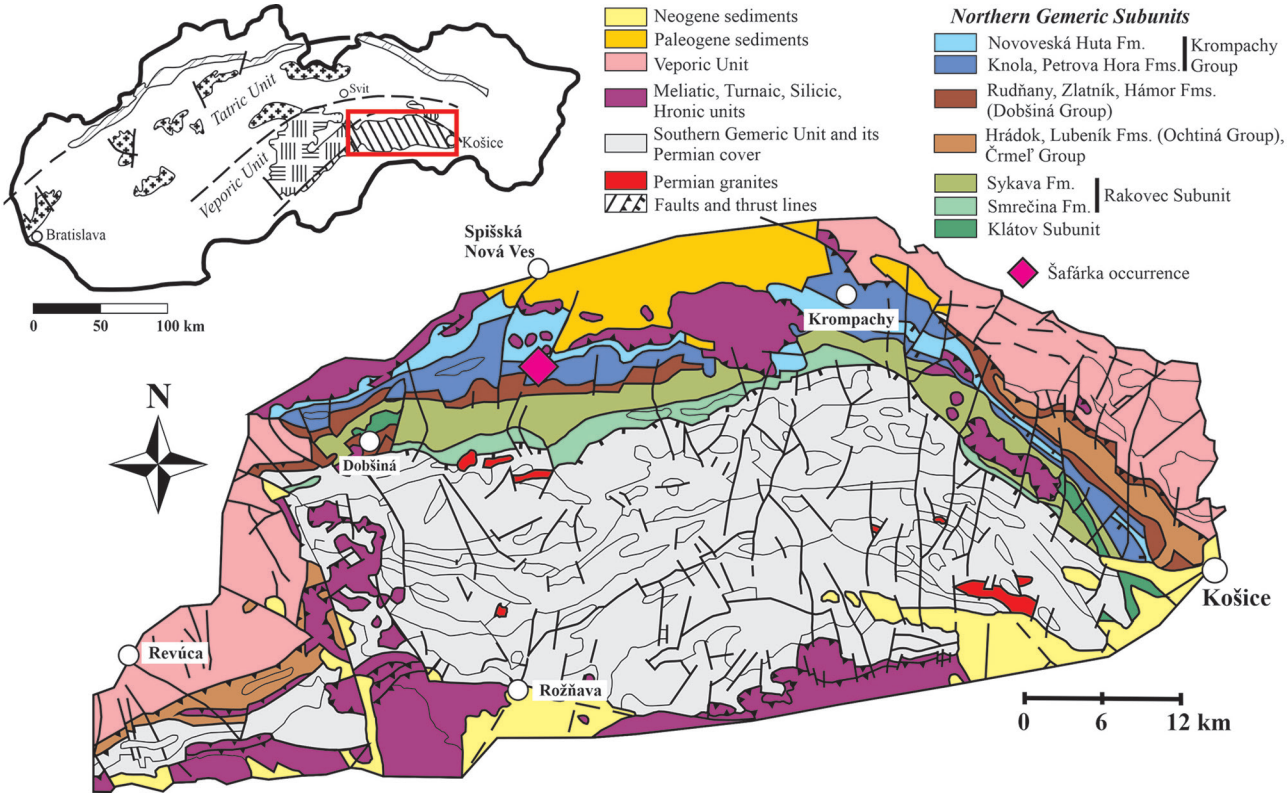

Fig. 1. Geological scheme of the Gemeric Unit (modified after Vozárová et al., 2014 and Mello et al., 2008).

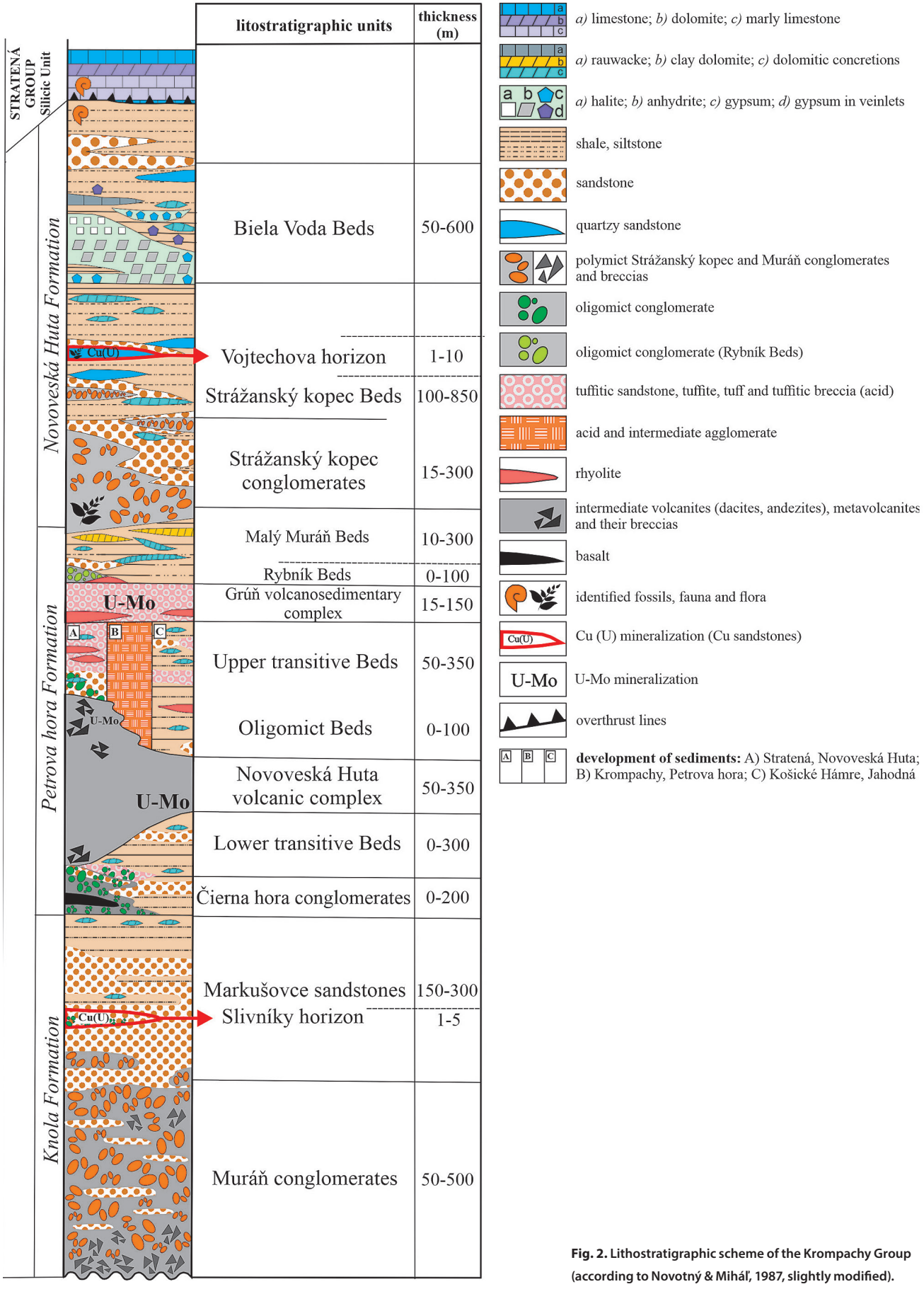

Fig. 2. Lithostratigraphic scheme of the Krompachy Group (according to Novotný & Miháľ, 1987, slightly modified).

locality (in some works named as the occurrence of Trubačovec). The upper, Vojtechova horizon lies in the Novoveská Huta Formation and forms part of the Strážanský kopec Beds (irregular, lenticular development of fine-grained green and green-greyish sediments). Copper sandstones of the Vojtechova horizon are located in the Suchá hora (Strážanský kopec), Malý Muráň, Medvedia hlava, Vojtechova osada (wider surroundings of Novoveská Huta) and at Stratená occurrences (Novotný & Mihál', 1987; Grecula et al., 1995).

Mineralogy of copper sandstones in the Gemeric Unit is given in the works of Ondrejkovič et al. (1964), Drnzík (1965), Grecula et al. (1995), Řídkošil (1977; 1978; 1981; 2007), Rojkovič (1997; 2003) and Števko (2014). The following primary and supergene minerals were found within the mineralisation of the copper sandstone type: ankerite, calcite, siderite, arsenopyrite, hematite, chalcopyrite, tetrahedrite, tennantite, bornite, pyrite, cobaltite, chalcocite, covellite, digenite, cuprite, wittichenite, enargite, gold, uraninite, U-Ti oxides, baryte, barium-pharmacosiderite, brochantite, langite, malachite, azurite, cinnabar, chalcophyllite, chrysocolla, clinoclase, cornwallite, zeunerite, metazeunerite, olivenite, posnjakite, strashimirite, tangdanite, tenorite, tyrolite, and goethite.

The Šafárka occurrence is located about 4 km SE of Novoveská Huta (part of Spišská Nová Ves district town), 300 m SE of Šafárka settlement, 500 m NE of the eastern peak of Trubačovec hill (also known as Altenberg hill; altitude 872 m asl.). The geographical coordinates of the occurrence are N 48.88°; E 20.56°.

The occurrence of copper sandstones at the Šafárka was the subject of a geological survey in the second half of the 20th century (Ondrejkovič et al., 1964). The locality was investigated by light technical works (exploration trenches and shafts) and by metallometric profiling. An old gallery (exploration name "Al Cu-1") was also recovered here. The results of the geological survey were negative. Mineralisation has a very irregular distribution, the individual mineralised bodies have a small directional range and the Cu content greatly varies (average 1 – 1.5 %; content dispersion 0.35 – 5.6 %). Mineral raw reserves have not been verified. At the locality, fine-grained yellow-brown sandstones are mineralised. The mineralised body is ENE to E trending, dipping 28 – 35° N to WNW and approximately 0.5 m thick. The main ore body is locally accompanied by overlying and underlying mineralised horizons at a distance of 2 m. The following minerals have been identified at the Šafárka occurrence: chalcopyrite, tetrahedrite, tennantite, bornite, pyrite, chalcocite, cinnabar, covellite, goethite, and malachite (Ondrejkovič et al., 1964; Grecula et al., 1995; Rojkovič, 1997; Rojkovič, 2003.

3. METHODS USED

Samples with increased radioactivity were searched in the gallery dump and in the forest road, using an SGR scintillation detector (sample activity measured in nSv/h), with a measuring range of 400 – 3000 keV and a measurement step of 0.2 s. Polished thin sections were observed in both, reflected and transmitted light on a Nikon ECLIPSE LV 100 POL polarising microscope (Faculty of Natural Sciences UMB, Banská Bystrica).

The chemical composition of minerals was determined using an electron microanalyser Jeol-JXA-8530F (Institute of Earth Sciences SAS, Banská Bystrica). The microanalyser was used to determine chemical composition of minerals using energy-dispersive spectrum (EDS) and for point wave-dispersion microanalysis (WDS). WDS microanalyses were performed under the following conditions: accelerating voltage 15 kV, measuring current 15 nA (uranophane) and accelerating voltage 20 kV, measuring current 15 nA (sulphides). The diameter of the electron beam ranged from 2 to 10 μm, ZAF correction was used. The following elements (crystal, X-ray lines) were analysed using these standards: Ag (PETL, L_α) – Ag, Fe (LIFL, K_α) – pyrite, Sb (PETL, L_α) – stibnite, Hg (PETL, M_α) – cinnabar, As (TAP, L_β) – GaAs, arsenopyrite, Se (TAP, L_β) – Bi_2Se_3, Bi (PETH, M_α) – Bi_2S_3, Cu (LIFH, K_α) – chalcopyrite, Ni (LIFH, K_α) – gersdorffite, Co (LIFH, K_α) – Co, S (PETJ, K_α) – pyrite, Zn (LIF, K_α) – sphalerite, Cd (PETJ,

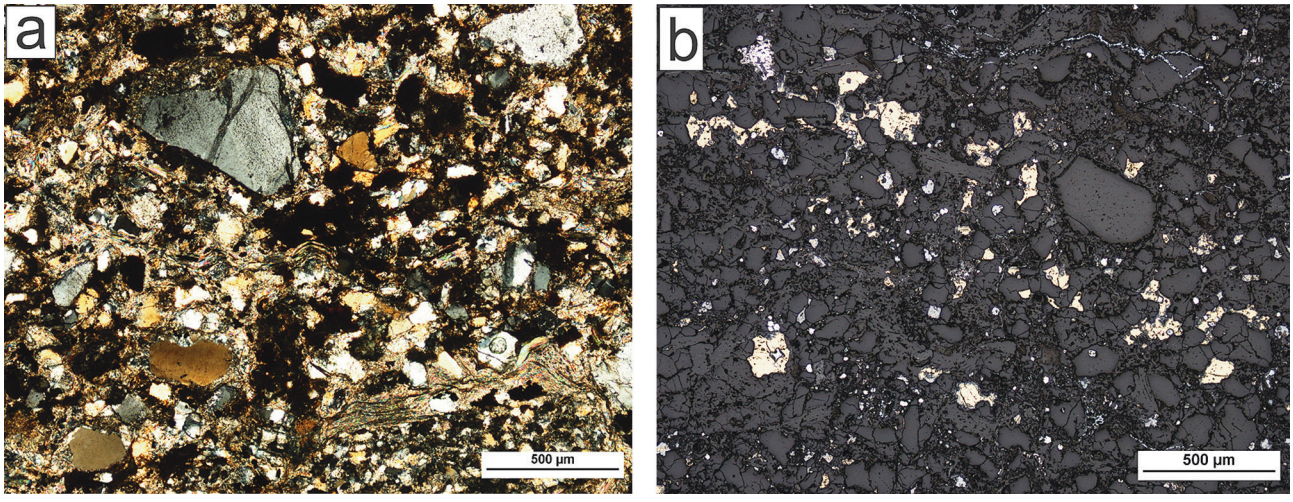

Fig. 3. Microphotographs of mineralisation: a) the mineralised sandstone. In the rock predominate fragments of quartz, less common is muscovite, and rock matrix is mostly sericitic; transmitted light, XPL; b) disseminated ore mineralisation in copper sandstones. Chalcopyrite (yellow), pyrite (white), chalcocite and goethite (both grey); reflected light, PPL. Photos: Š. Ferenc.

L_α) – CdTe, Pb (PETJ, M_α) – galena, Au (PETH, M_α) – Au, Mn (LIFH, K_α) – rhodonite, Ca (PETL, K_α) – diopside, Ba (PETL, L_α) – baryte, Mn (LIFL, K_α) – rhodonite, Na (TAP, K_α) – albite, K (PETL, K_α) – ortoclase, U (PETL, M_β) – UO_2, Mg (TAP, K_α) – diopside, P (PETL, K_α) – apatite Al (TAP, K_α) – albite, Si (TAP, K_α) – plagioclase An_{65}, Fe (LIFH, K_α) – hematite, Sr (PETH, L_α) – celestite. The detection limit for individual elements ranged from 0.003 – 0.03 wt. %. Elements whose content values are below the detection limit are not included in the tables below. Photo documentation of the minerals and their microstructural interrelationships was carried out in the backscattered electron (BSE) mode on the same instrument.

Distribution maps of individual elements were made using X-ray fluorescence spectroscopy (XRF) on M4 Tornado, Bruker (Institute of Earth Sciences SAS, Banská Bystrica). The rhodium target X-ray tube was operating at conditions: current 50 kV, voltage 600 V, measuring range 40 KeV/130 kcps. The instrument is equipped with an XFlash silicon drift X-Ray detector (SDD). Maps were constructed with a 25 µm spot size and with 50 µm pixel size and a dwell time of 5 ms/pixel. Analyses were carried out under the vacuum. The XRF element maps were generated with XRF software.

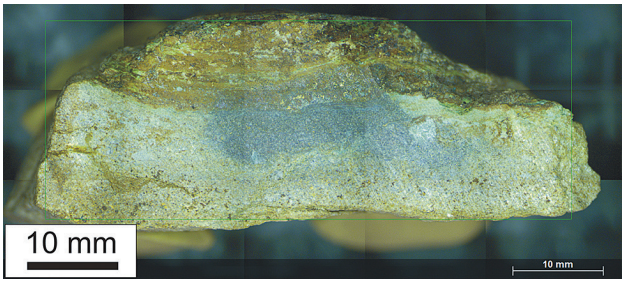

Fig. 4. Macro view of a mineralised sandstone. In the central part, the colour of the rock is grey (with small grains of yellow chalcopyrite), because it is not affected by supergene alteration (limonitisation). The marginal limonitised parts are yellow-brown to brown. Photo: J. Vlasáč.

4. RESULTS

4.1. Host rock and mineralisation nature

Copper-uranium mineralisation occurs in fine-grained psammites (Fig. 3a). The average grain size ranges from 0.1 to 0.3 mm, occasionally even 3 mm. Non-weathered rock is a greenish-grey in colour. The surface of the samples is yellow-brown, coloured by weathering (limonitisation), with coatings of green supergene minerals of Cu and U. Radioactivity of the samples ranged from 530 to 700 nSv/h.

The main rock-forming mineral is mono- and polycrystalline quartz, which forms angular to subangular grains. Carbonate (probably authigenic), muscovite and fragments of sericite schists or highly altered volcanics are present to a lesser extent. Accessory minerals represent K-feldspar, tourmaline and more

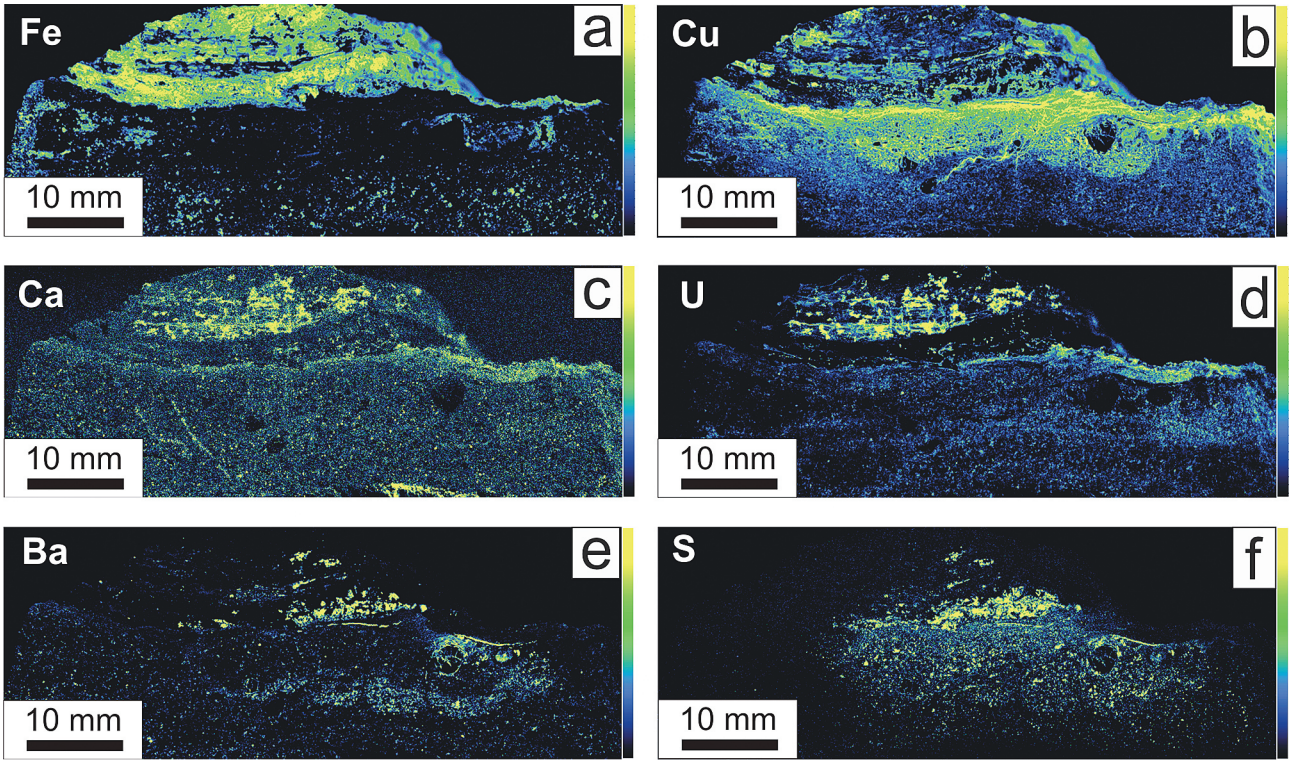

Fig. 5. XRF map of selected elements distribution: a) Iron is mainly bound to goethite (compare with Fig. 4) and partly to chalcopyrite. b) Copper is bound mostly to malachite and to chalcopyrite. c) Calcium is bound mostly to uranophane-α in the limonitised part of the sample (compare with Fig. 4). d) Uranium is mainly bound to uranophane and its distribution corresponds to those of Ca (compare Fig. 5c). e) Barium is mainly bound to baryte in the limonitised part of the sample (compare Fig. 4). f) Sulphur is bound partly to baryte (compare Fig. 5d) and partly to Cu-Fe sulphide minerals (compare Fig. 5 a, b). The relative content of the element increases from the black end of the colour scale to the yellow. Photo: J. Vlasáč.

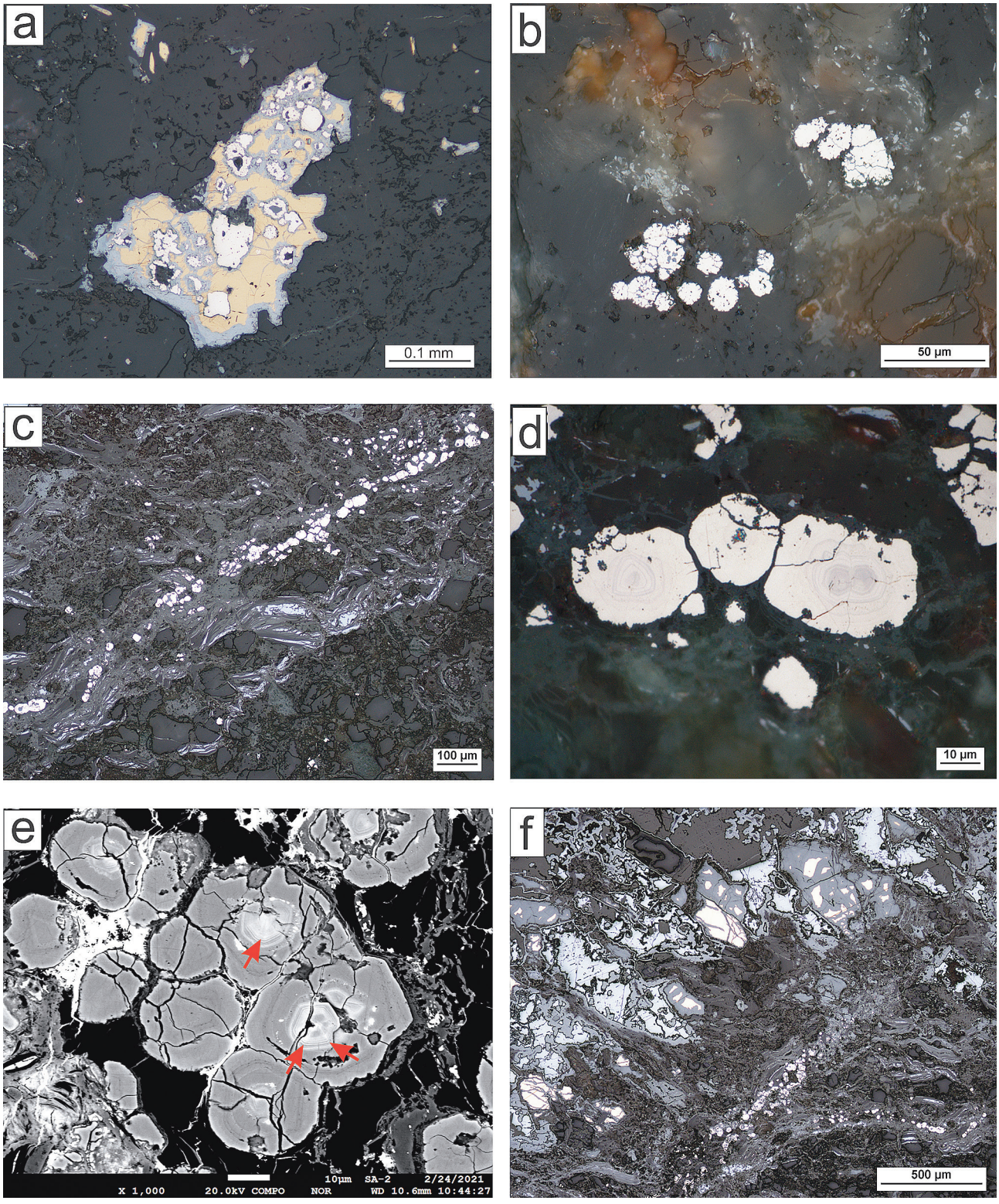

Fig. 6. Microphotographs of minerals: a) Chalcopyrite (yellow) encloses pyrite grains (white). Chalcopyrite-pyrite aggregate is replaced by chalcocite (grey, bluish tint) along the edges and cracks. b) Clusters of spherical pyrite aggregates (white) are particularly replaced by goethite (grey) in sandstone. c) Veinlet consists of hypidiomorphic to idiomorphic pyrite crystals in sandstone. Chalcocite is grey with a bluish tint. d) Zonal pyrite – *bravoite*. The brownish zones are enriched with Ni and Co. e) Zonal pyrite – *bravoite*. The light zones are enriched with Ni and Co. The white phase represents the supergene mineral of Ba-U-Ti-Fe-S, or an intimate mixture of supergene minerals of these elements. Red arrows indicate places with visible preferential Ni concentration at the edges of the incremental zones (lighter bands across the crystal following the angles of incremental zones). f) Chalcopyrite (yellow) in association with chalcocite (light grey, blue tint) in a mineralised rock. Both minerals are replaced and enclosed by goethite (dark grey). Pyrite (white) forms accumulations at the bottom of the image. Note: a-d, f) – reflected light, PPL, photo: Š. Ferenc; e) BSE picture, photo: T. Mikuš.

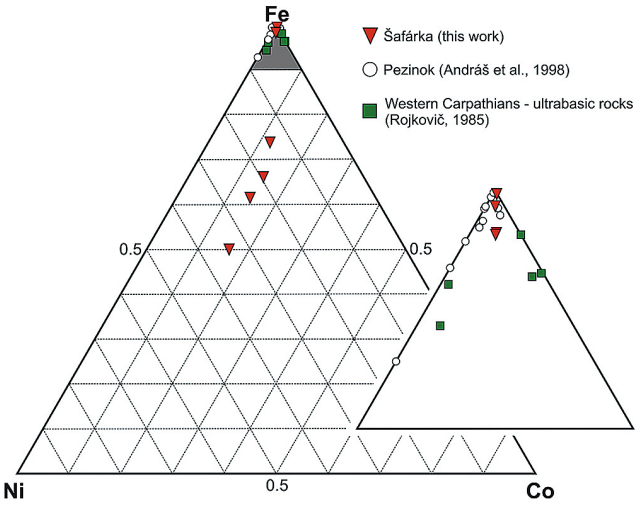

Fig. 7. Microanalyses (in apfu) of pyrite (*bravoite* respectively) in the ternary diagram of the Fe-Ni-Co system.

or less leucoxenised Fe-Ti oxides. Rock matrix consists mainly of sericite and fine-grained quartz.

Ore minerals form disseminations and veinlets in sandstones (Fig. 3b). Supergene minerals of Fe, Cu, and U fill microscopic cavities and cracks in the rock. The distribution of individually selected elements in the rock sample (Fig. 4) is shown on XRF maps (Fig. 5a-f).

4.2. Primary minerals

The association of primary minerals is very simple and monotonous in contrast to the association of supergene minerals. Primary sulphide minerals in the studied samples are mainly chalcopyrite, less widespread is pyrite and rarely tennantite-(Fe). The only primary uranium-bearing mineral phase (U^{4+}) present at the site is uranium-bearing *leucoxene*.

Chalcopyrite is the main ore mineral. It forms irregular grains and aggregates up to 1 – 2 mm in size, scattered in the rock and encloses pyrite grains. From the margins of the aggregates and along the cracks, chalcopyrite is to a variable degree, usually replaced by chalcocite and goethite (Fig. 6a,f). Its chemical composition has only been determined by non-standardised EDS analyses and corresponds to the ideal formula of this mineral phase.

Pyrite is relatively widespread but less so than chalcopyrite. It forms irregular but also isometric grains (up to 0.1 mm) in the rock or enclosed in chalcopyrite (Figs. 3a, 6a). Locally also forms clusters of spherical aggregates 10 – 15 μm in size in the sandstone (Fig. 6b). Hypidiomorphic to idiomorphic pyrite crystals are sometimes arranged in thin veins 2 – 3 mm long (Fig. 6c). Optical zoning of some crystals (variety *bravoite*) was observed in these veins due to a different content of admixtures, mainly Ni and Co (Fig. 6d,e). Pyrite is replaced to varying degrees by goethite. The chemical composition of pyrite from the Šafárka occurrence (Tab. 1; Fig. 7) is characterised by the wide variability of Fe (0.48 – 0.98 apfu), Ni (up to 0.32 apfu) and Co (up to 0.15 apfu) content. Nickel and cobalt have a positive correlation with each other and at the same time both elements show a negative correlation with Fe, according to the works of Riley (1965, 1968). A stable admixture is As, whose content is usually between 0.01 – 0.02 apfu. In one case, an anomalous increased As content was found (0.11 apfu; Tab. 1, analyse 6). The Cu and Sb content is negligible.

Tennantite-(Fe) was found only very sporadically in studied samples. It forms relics (up to 50 μm in size) in goethite. Its chemical composition was determined by non-standardised EDS analyses. Only, the increased Hg content (up to 7.4 wt. %)

Tab. 1. Chemical composition of pyrite (bravoite) from the Šafárka occurrence.

an.	1	2	3	4	5	6	7	8
Fe	21.70	27.51	29.50	32.53	44.82	44.85	45.15	45.29
Co	7.21	6.72	6.74	5.44	0.42	0.07	0.42	0.15
Ni	15.46	11.35	9.08	6.56	0.42	0.00	0.46	0.15
Cu	0.82	0.33	0.33	0.36	0.44	0.24	0.67	0.53
As	0.62	1.23	0.90	0.99	1.02	6.81	0.35	0.78
Sb	0.11	0.01	0.12	0.22	0.17	0.34	0.16	0.27
S	53.21	53.06	53.90	53.68	53.55	49.11	52.15	53.08
Total wt. %	99.12	100.22	100.57	99.78	100.84	101.42	99.36	100.24
atomic proportions (calculated on the basis of 3 atoms)								
Fe	0.475	0.597	0.635	0.704	0.960	0.990	0.983	0.976
Co	0.149	0.138	0.137	0.112	0.009	0.001	0.009	0.003
Ni	0.322	0.234	0.186	0.135	0.008	0.000	0.009	0.003
Cu	0.016	0.006	0.006	0.007	0.008	0.005	0.013	0.010
As	0.010	0.020	0.014	0.016	0.016	0.112	0.006	0.013
Sb	0.001	0.000	0.001	0.002	0.002	0.003	0.002	0.003
S	2.027	2.005	2.020	2.024	1.997	1.888	1.978	1.993
Cat.	0.962	0.975	0.964	0.958	0.985	0.996	1.014	0.992
Fe/Σ Cat.	0.49	0.61	0.66	0.74	0.97	0.99	0.97	0.98
Cat/S+As+Sb	0.47	0.48	0.47	0.47	0.49	0.50	0.51	0.49

Tab. 2. Microprobe analyses of Cu-S mineral phases yarrowite (Yar) and chalcocite (Cc) from the Šafárka occurrence.

an.	1	2	3	4
mineral	Yar	Cc	Cc	Cc
Ag	0.02	0.01	0.02	0.06
Cu	68.67	78.90	78.42	79.18
Mn	0.03	0.00	0.01	0.02
Fe	0.19	0.96	0.73	2.83
Hg	0.00	0.03	0.06	0.04
Pb	0.10	0.07	0.12	0.04
S	30.63	20.95	20.74	19.71
Total wt. %	99.64	100.92	100.09	101.87
atomic proportions				
Ag	0.001	0.000	0.000	0.001
Cu	9.003	1.947	1.953	1.954
Mn	0.004	0.000	0.000	0.000
Fe	0.029	0.027	0.021	0.079
Hg	0.000	0.000	0.000	0.000
Pb	0.004	0.001	0.001	0.000
S	7.959	1.025	1.024	0.964
Cat.	9.041	1.975	1.976	2.036
Cat/S	1.14	1.93	1.93	2.11

Atomic proportions were calculated on the basis of 17 atoms (yarrowite) and 3 atoms (chalcocite).

is more interesting. Rojkovič (1997) describes tennantite-(Hg) with Hg content of up to 16.6 wt. % (1.40 apfu) at the Šafárka occurrence.

Uranium bearing leucoxene forms fuzzy accumulations of allotriomorphic grains up to 5 μm in size, or veinlets (in shear microzones), up to 0.1 mm thick in the rock (Fig. 11b).

4.3. Supergene minerals

The studied samples with Cu-(U) mineralisation were significantly influenced by supergene processes, which was reflected in a diverse range of secondary minerals. Cementation minerals are represented by chalcocite and yarrowite, while uranophane-α, malachite, goethite, baryte, anglesite, and cinnabar were formed in the oxidation zone.

Chalcocite is, together with chalcopyrite, the most abundant ore mineral. It forms irregular aggregates up to 1 mm in size. It replaces aggregates of chalcopyrite (sometimes even completely) along the margins and cracks and is enclosed by goethite (Fig. 6a,f). The chemical composition of chalcocite from the Šafárka is homogeneous and close to the ideal formula of this mineral phase (Tab. 2). From the admixtures, only Fe reaches a maximum of 0.08 apfu. Based on 3 WDS analyses, the average chemical composition of the studied chalcocite can be expressed by an empirical formula $(Cu_{1.95}Fe_{0.04})_{\Sigma 1.99}S_{1.00}$.

Yarrowite has been identified very rarely. It forms grains up to 20 μm in goethite. The studied yarrowite contains only minimal amounts of admixtures (Tab. 2) and its chemical composition corresponds to the empirical formula $(Cu_{9.00}Fe_{0.03})_{\Sigma 9.03}S_{7.96}$.

Uranophane-α is abundant in the investigated samples, especially in the limonitised marginal parts of the samples (compare Fig. 5a,d). It appears in fissures or forms fillings of small

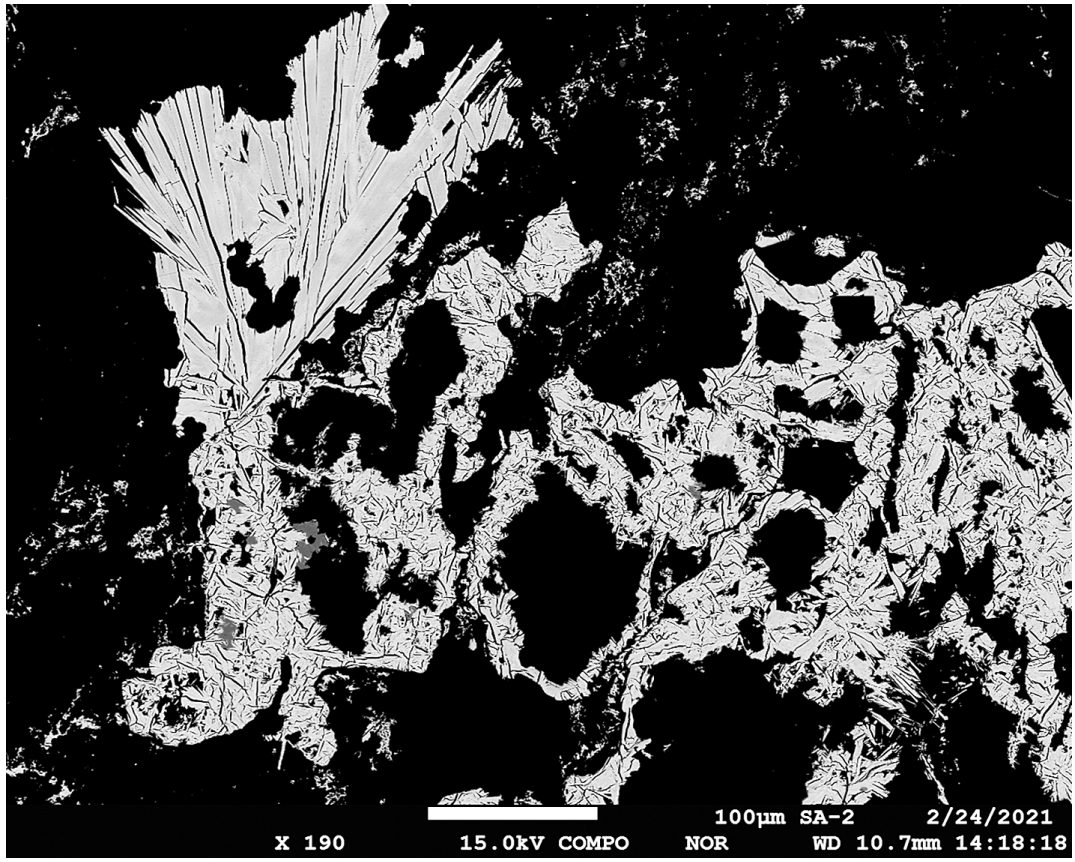

Fig. 8. Aggregates of uranophane II crystals (light grey) in limonitised rock. In BSE mode, uranophane I and II cannot be recognised due to their same chemical composition. BSE picture, photo T. Mikuš.

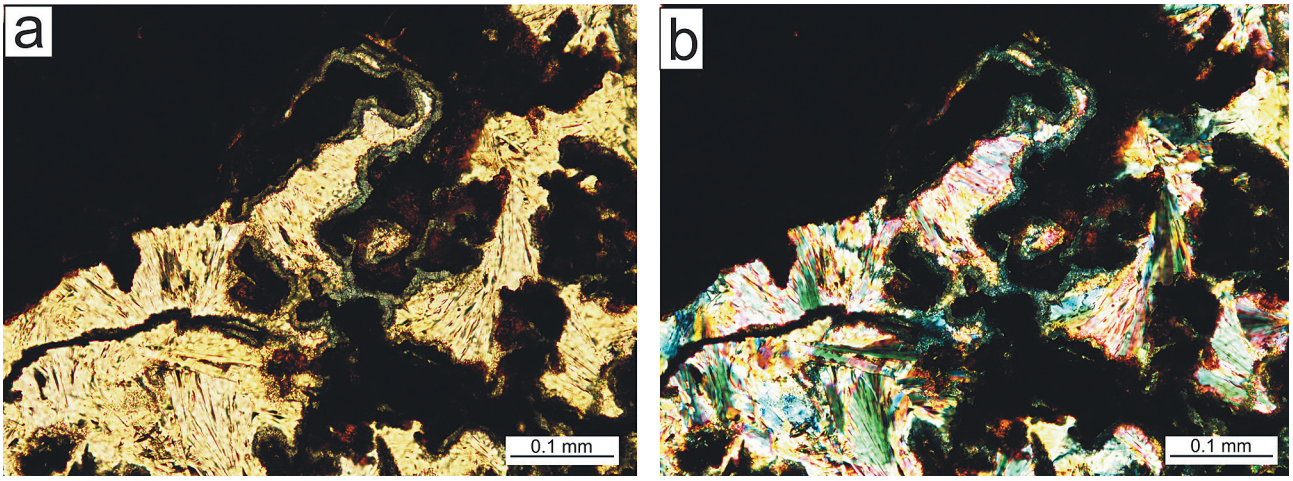

Fig. 9. Microphotographs of minerals: a) Uranophane-α in the cavity of limonitised rock. Aggregates of light yellow uranophane II with fine, but visible pleochroism. The aggregates are locally rimmed with uranophane I (bluish colour). Transmitted light, PPL. b) Interference colours of uranophane from the previous picture. Transmitted light, XPL. Photo Š. Ferenc.

Tab. 3. Representative microanalyses of uranophanes-α from the Šafárka occurrence.

an.	1	2	3	4	5	6	7	8	9	10
K_2O	0.10	0.06	0.07	0.08	0.09	0.12	0.11	0.15	0.07	0.11
CaO	6.67	6.64	6.73	6.32	6.76	6.80	6.66	6.70	6.71	6.43
BaO	0.00	0.00	0.24	0.00	0.13	0.24	0.84	0.82	0.09	0.55
FeO	0.03	0.31	0.08	0.26	0.11	0.00	0.07	0.11	0.01	0.20
CuO	0.03	0.04	0.01	0.63	0.39	0.10	0.20	0.08	0.14	0.44
ZnO	0.01	0.00	0.00	0.06	0.00	0.01	0.30	0.13	0.15	0.00
TiO_2	0.15	0.00	0.21	0.13	0.00	0.00	0.00	0.00	0.11	0.04
SiO_2	13.06	13.36	12.89	12.78	12.62	13.25	13.50	13.30	13.66	13.09
P_2O_5	0.42	0.28	0.49	0.09	0.79	0.58	0.39	0.25	0.38	0.63
As_2O_5	0.06	0.09	0.05	0.00	0.22	0.09	0.00	0.00	0.00	0.27
SO_3	0.05	0.00	0.00	0.02	0.01	0.14	0.35	0.20	0.00	0.01
UO_3	67.88	68.24	68.63	69.23	68.98	69.15	68.60	69.61	70.33	70.86
H_2O*	11.88	11.91	11.81	11.73	11.80	11.88	11.99	11.85	11.86	11.72
Total wt. %	100.33	100.93	101.20	101.32	101.90	102.35	103.01	103.20	103.51	104.34
atomic proportions (calculated on the basis of 5 atoms)										
K	0.009	0.005	0.006	0.007	0.008	0.011	0.010	0.013	0.006	0.010
Ca	1.023	1.008	1.026	0.966	1.027	1.020	0.983	0.996	0.994	0.956
Ba	0.000	0.000	0.013	0.000	0.007	0.013	0.045	0.045	0.005	0.030
Fe	0.003	0.037	0.010	0.031	0.013	0.000	0.008	0.013	0.001	0.023
Cu	0.003	0.005	0.001	0.068	0.042	0.011	0.020	0.008	0.015	0.046
Zn	0.001	0.000	0.000	0.006	0.000	0.001	0.030	0.013	0.016	0.000
Ti	0.016	0.000	0.022	0.014	0.000	0.000	0.000	0.000	0.011	0.004
Si	1.870	1.893	1.836	1.825	1.791	1.856	1.860	1.846	1.888	1.817
P	0.025	0.017	0.029	0.005	0.047	0.034	0.023	0.015	0.022	0.037
As	0.002	0.003	0.002	0.000	0.008	0.003	0.000	0.000	0.000	0.010
S	0.005	0.000	0.000	0.002	0.001	0.015	0.036	0.021	0.000	0.001
U	2.041	2.032	2.054	2.076	2.055	2.035	1.985	2.030	2.043	2.066
H_2O*	5.000	5.000	5.000	5.000	5.000	5.000	5.000	5.000	5.000	5.000
Cat.	1.056	1.055	1.079	1.092	1.098	1.056	1.097	1.088	1.047	1.069
An.	1.903	1.913	1.867	1.832	1.847	1.909	1.919	1.882	1.910	1.865
Cat/U	0.52	0.52	0.53	0.53	0.53	0.52	0.55	0.54	0.51	0.52
Cat/An	0.55	0.55	0.58	0.60	0.59	0.55	0.57	0.58	0.55	0.57
U/An	1.07	1.06	1.10	1.13	1.11	1.07	1.03	1.08	1.07	1.11

The empirical formula of uranophane was calculated on the basis of 5 atoms. H_2O* content was calculated on the basis of the uranophane ideal formula and charge balance.

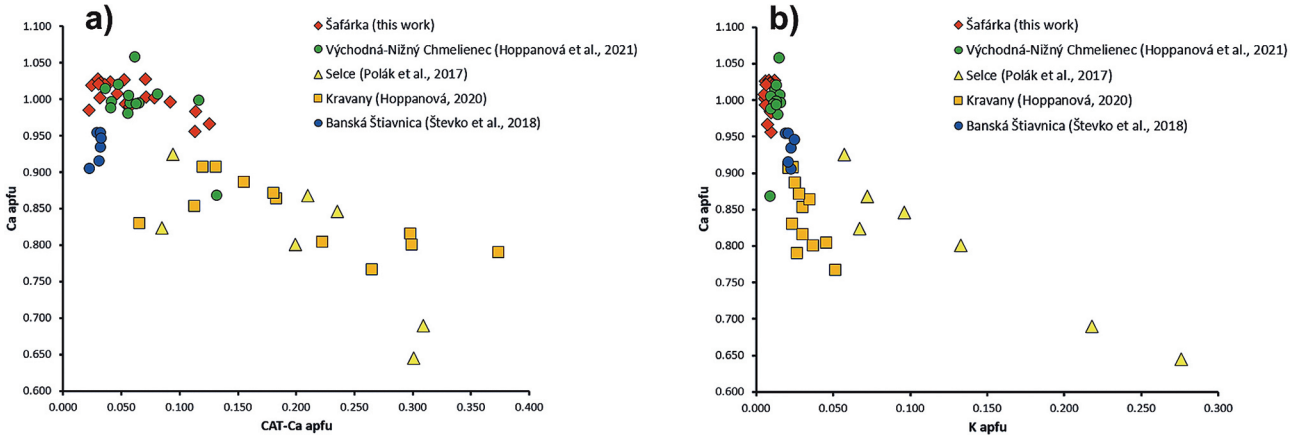

Fig. 10. The mutual relationship of calcium and the other elements (cationic position) in uranophanes from Slovakia. a) Ca vs other elements (Fe, Cu, Ba, Mg, K, Ti, etc.), b) Ca vs K.

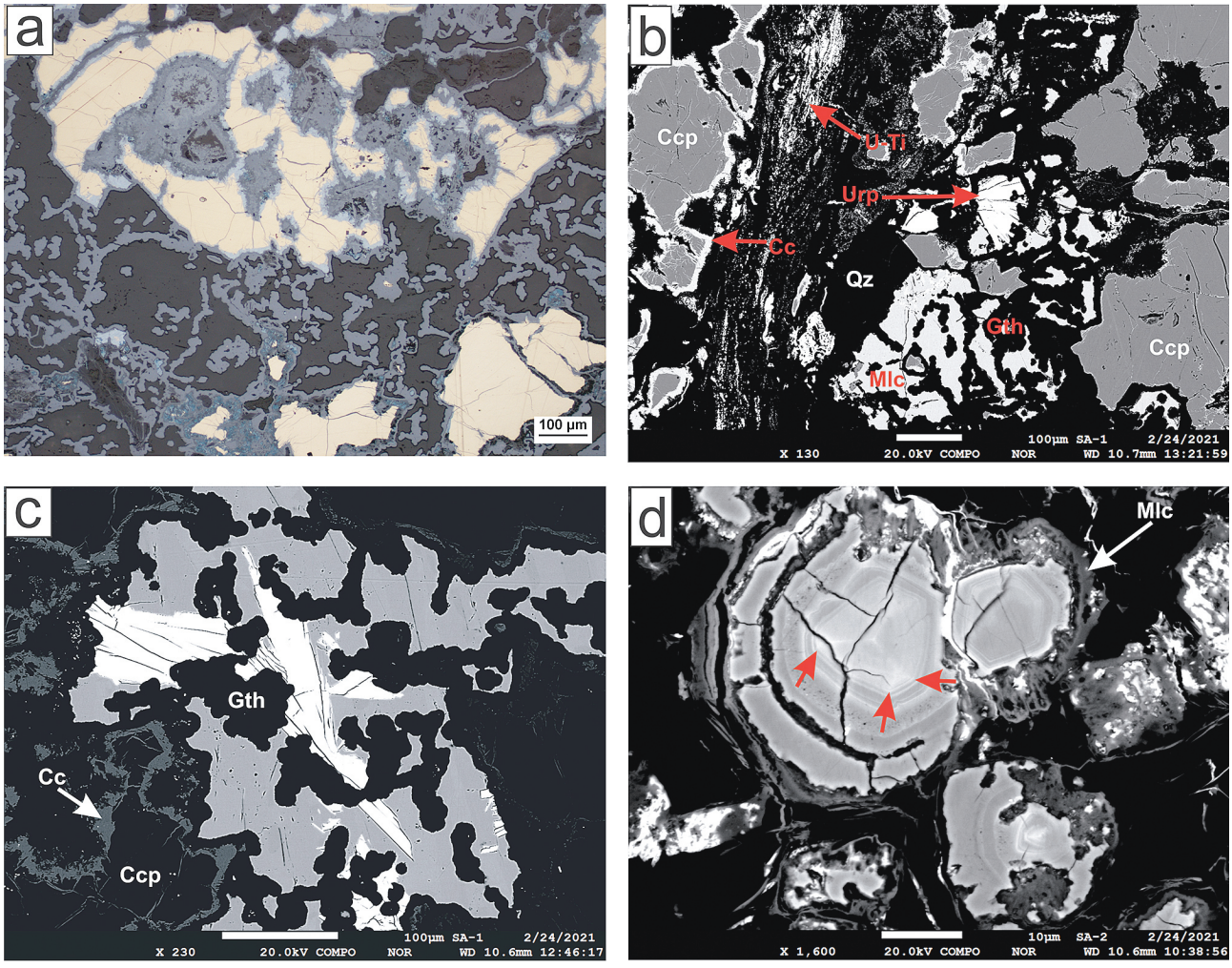

Fig. 11. Microphotographs of minerals: a) Chalcocite (light grey) rims chalcopyrite aggregate (yellow) along the edges and fissures. Both of them are overgrown by goethite (dark grey). Isometric cavities in chalcopyrite aggregate (top of picture) filled by goethite represent complete pseudomorphoses after original pyrite (compare Fig. 6a). b) Chalcopyrite (Ccp) aggregates are rimmed by chalcocite (Cc). Malachite (Mlc) is overgrown with goethite (Gth, black) and cut by uranophane-α veinlets (white). Uranophane (Urp) also forms cavity fills in goethite. U-bearing *leucoxene* (U-Ti) form fine-grained, disseminated irregular aggregates, veinlets respectively in limonitised rock. c) Baryte (light grey) intergrows with goethite (Gth) and overgrows on uranophane aggregates (white). Accompanying minerals are chalcopyrite (Ccp) rimmed by chalcocite (Cc). d) The zonal crystal of pyrite (var. *bravoite*) is (partially selective) corroded by malachite (Mlc, dark grey). Malachite is locally intergrown with baryte (white). Red arrows indicate places with visible preferential Ni concentration at the edges of the *bravoite* incremental zones (lighter bands across the crystal following the angles of incremental zones). a) – Reflected light, PPL, photo: Š. Ferenc; b-d) – BSE pictures, photo: T. Mikuš.

cavities (size up to 0.5 mm) in sandstones. Two generations of uranophane-α can be distinguished in the transmitted light. Uranophane I forms thin, small-crystalline rims along the walls of the cavities, the central parts of those are filled with irregular or fan-shaped aggregates of acicular uranophane II crystals (length up to 0.2 mm; Fig. 8). It is found in association (resp. supergene oxidation paragenesis) with goethite, malachite, baryte, and rarely with anglesite. In the transmitted light (PPL; Fig. 9a) uranophane II is anisotropic, white-yellow, with indistinct pleochroism (white-yellow – deeper shade of yellow) and bright interference colours (XPL; Fig. 9b). The chemical composition of uranophane I and II are the same and relatively homogeneous (Tab. 3; Fig. 10). In the cationic position (except the main constructional element – calcium), only Fe (up to 0.04 apfu), Ba (up to 0.05 apfu) and Cu (up to 0.07 apfu) are relatively important. From Fig. 10a, it can be seen that the total content of the other elements (except calcium) does not exceed 0.15 apfu in the case of uranophane from the Šafárka site. In addition to Si, accessory P (up to 0.05 apfu) is stably present in the anionic position; sporadically, slightly increased As (up to 0.01 apfu) and S (up to 0.04 apfu) contents were detected. Compared to uranophanes-α from other Slovak localities (Fig. 10), uranophane from the Šafárka belongs to relatively pure, "high calcium" mineral phases, similarly to uranophane from Banská Štiavnica (Števko et al., 2018), or Východná (Hoppanová et al., 2021). Substitution of other cations for Ca (up to ~ 0.40 apfu; Fig. 10b) enforced in uranophane from the Kravany uranium deposit (Hoppanová, 2020) and from Selce occurrence (Polák et al., 2017). Uranophane from Selce, in contrast to uranophane from other Slovak localities, shows a more pronounced "boltwoodite" substitution K → Ca (up to ~ 0.30 apfu; Fig. 10b). The average chemical composition of uranophane-α (10 WDS analyses; Tab. 3) from the Šafárka occurrence is characterised by the empirical formula $(Ca_{1.00}Ba_{0.02}Cu_{0.02}K_{0.01}Fe_{0.01}Zn_{0.01}Ti_{0.01})_{\Sigma 1.08}(UO_2)_{2.04}[(SiO_3OH)_{1.85}(PO_4)_{0.03}(SO_4)_{0.01}]_{\Sigma 1.89}(H_2O)_5$.

Goethite is very abundant in the studied samples and makes brownish-yellow and brown colouration of sandstones. It forms dense accumulations of irregular aggregates and veinlets (often with optical zonation) in the rock, replacing the sandstone matrix. It replaces pyrite and chalcopyrite grains and aggregates (often complete pseudomorphoses) over cracks and edges; Fig. 11a), and also encloses chalcocite aggregates (Fig. 6f). The chemical composition of goethite has not been studied.

Malachite is an abundant mineral, especially in the marginal and limonitised parts of the studied samples. It forms cryptocrystalline coatings on sandstone cracks or fills small cavities in the rock (size up to 0.5 mm). It most commonly overgrows with goethite (cavity filling), less often with uranophane (Fig. 11b) and other supergene minerals, respectively. Locally malachite corrodes pyrite (*bravoite*). The chemical composition of malachite has not been investigated in detail. According to non-standardised EDS analyses, malachite from the Šafárka occurrence contains up to 2 wt. % Fe.

Baryte is a relatively abundant mineral. It forms irregular aggregates up to 0.5 mm in size. It fills the cavities in goethite and overgrows the uranophane-α aggregates (Fig. 11c). It rarely overgrows with malachite and encloses pyrite crystals (Fig. 11d). Baryte was determined only by non-standardised EDS analysis.

Anglesite is relatively rare. It forms irregular aggregates (up to 0.5 mm in size) overgrown with fine-grained uranophane I. It was determined only by non-standardised EDS analysis.

Cinnabar belongs to the rarer mineral phases. It forms irregular aggregates in association with uranophane-α and other supergene minerals, which represents a product of weathering of tennantite-(Hg), or Hg-bearing tennantite-(Fe). It was determined only by non-standardised EDS analysis.

5. DISCUSSION AND CONCLUSIONS

5.1. Some notes on bravoite

Bravoite was first described by Hillebrand (1907) from Minasragra (Peru) and suggested its name in honour of the Peruvian mineralogist and deposit geologist José J. Bravo. It was considered a separate mineral species until 1989 when it was discredited by the International Mineralogical Association (webmineral.com). Nowadays, bravoite is considered a pyrite variety.

Bravoite formation is related to higher temperature igneous or hydrothermal conditions but also with low-temperature processes under the influence of meteoric fluids (Bernard et al., 1992). Therefore, it is widespread in many ore deposits of various genesis worldwide (mindat.com). This exciting variety of pyrite has also been found in several localities in Slovakia. Within the ore mineralisation of ultrabasic rocks, it was found in Pohronská Polhora, Ploské, and Sedlice (Rojkovič, 1985). In the filling of amygdale cavities of Permian basalts of the Hronic Unit near Poprad it was identified by Antaš (1963). In the Gemeric Unit, *bravoite* appears in quartz veins with Variscan(?) U mineralisation at Hnilec (Varček, 1977), also in Alpine siderite-sulphidic veins at Rožňava, Drnava, Medzev, Nižná Slaná (Varček, 1971), and Mníšek nad Hnilcom (Matula, 1969). However, the identification of *bravoite* from Slovakia is mainly based on optical studies, while its relevant chemical analyses have not yet been published.

On the basis of its chemical composition, pyrite from the Šafárka can be divided into several groups: a) pyrite with a minimum content of admixtures, with composition almost corresponding to the formula FeS_2 (Tab. 1; an. 5, 7, 8); b) As-bearing pyrite (Tab. 1; an. 6), with chemical composition $Fe_{0.99}(As_{0.11}S_{1.89})_{\Sigma 2.00}$; and c) *bravoite* (Tab. 1; an. 1 – 4) with compositional extent $(Fe_{0.47}Co_{0.15}Ni_{0.32}Cu_{0.02})_{\Sigma 0.96}S_{2.03}$ to $(Fe_{0.70}Co_{0.11}Ni_{0.14}Cu_{0.01})_{\Sigma 0.96}S_{2.02}$.

Arsenic, together with Se, Te, and Sb, most often enters the anionic position of pyrite, at the expense of the S content, with the $As^{1-} \rightarrow S^{1-}$ substitution being the most prevalent (e.g., Fleet & Mumin, 1997 and citation therein). Arsenic can also enter the cationic position of pyrite by substitution $As^{3+} \rightarrow Fe^{2+}$ (Deditius et al., 2008; Quian et al., 2013). The As content in natural pyrite can vary, from trace amounts to almost 10 wt. % (Abriatis et al., 2004; Bowles et al., 2001; Majzlan et al., 2014), in the synthetic pyrite up to ~ 19 wt. % (Qian et al., 2013). However, at high contents (determined from microprobe analyses), As may be present in pyrite in solid solution, or the high content may be due to the overgrowth of arsenopyrite and pyrite nanoparticles,

or nano-inclusions of amorphous As-Fe-S phase may also be present in pyrite (Deditius et al., 2009). Theoretical calculations (Reich & Becker, 2006) indicate that pyrite may contain up to ~ 6 wt. % As in solid solution, before its decomposition into pyrite + arsenopyrite. Except for one analysis (Tab. 1; an. 6), arsenic is stably present in the studied pyrite and *bravoite* from the Šafárka occurrence (averagely 0.84 wt. %; 0.01 apfu As). However, based on the small number of analyses, it is impossible to determine which style of the substitutions as mentioned above is involved (*sensu* Zhang et al., 2022). In the case of the studied occurrence, As most likely enters the anionic position because the substitution $As^{1-} \rightarrow S^{1-}$ is generally the most widespread, while the entry of As into the cationic position of pyrite has been found only rarely. In the studied pyrites (*bravoite*), arsenic is probably present in solid solutions.

The most common admixtures in pyrite are Ni and Co, less Cu entering the cationic position instead of Fe. A study of the chemical composition of natural Fe-Ni-Co-(Cu)-S phases in the FeS_2-NiS_2-CoS_2 system demonstrated the complete miscibility of solid solutions (Bayliss, 1989). Experimental research of the synthetic phases (above 400 °C) in turn indicates complete miscibility in this system rather along the FeS_2-CoS_2 and FeS_2-NiS_2 lines (Klemm, 1965), at the presence of an immiscibility field (~ 700 °C) between FeS_2 and NiS_2 (Clark & Kullerud, 1963; Karup-Møller & Makovicky, 1995). The chemical composition of pyrite (*bravoite*) from the Šafárka locality confirms the complete miscibility of solid solutions in the whole FeS_2-NiS_2-CoS_2 system, although the trend of analyses is parallel to the Fe-Ni axis of the ternary diagram (Fig. 7). Based on the Fe/(Fe + Ni + Co + Cu) ratio, the studied mineral phase can be considered as a *bravoite-(Fe)* (*sensu* Kostov & Mincheva-Stefanova, 1984).

A characteristic feature of *bravoites* is their optical zoning (both growth and sectoral) caused by the increased Ni and Co content in the mineral structure (ultimately, the optical zoning is the result of chemical zoning). For example, El Baz & Amstutz (1963) identified eight types of *bravoite* zoning in the Fredericktown sulphide ores (Missouri, USA). Such zoning reflects the selective distribution of elements, that is caused by differences in the morphology and charge of growth surfaces of the same age in the crystal (Watson, 1996). In the case of pyrite, these are mainly growth (also cleavage) surfaces of (100), (111), (110), and (210) (Rosso & Vaughan, 2006). A cubic pyrite crystallises most often in cubes and pentagonal dodecahedron, which in the case of an idiomorphic crystal allows its 3, 4, 5, 6 and 9 side cut contour. Nickel (Co, respectively) is preferably concentrated at the margins of the crystal/growth zone, while the faces are characterised by a higher Fe content, at the expense of Ni and Co content (Vaughan, 1969; Bhattacharyya et al., 2016). *Bravoites* from the Šafárka occurrence are mainly characterised by hexagonal contours of growth zones, with occasional near-triangular contours with rounded edges (Figs. 6d,e, 11d). Their zoning is caused predominantly by ranging in Ni content from 15.46 wt. % (0.32 apfu) to 6.56 wt. % (0.14 apfu) and the corresponding fluctuations in Fe content (negative correlation), at a relatively constant Co content (Tab. 1; Fig. 7). The studied *bravoites* represent a nice example of the preferred concentration of Ni at the edges of the crystals and growth zones, which stands out, especially in the study of the mineral phase in BSE mode on an electron microanalyser (Figs. 6e, 11d). Increased Ni content is manifested here by increasing white colour intensity (due to the presence of a heavier element).

5.2. About the presence of uranophane-α

In the Northern Gemeric Unit, copper sandstones of the Vojtechova (Suchá hora occurrence) and Slivníky horizons (Šafárka, Markušovská dolina) locally host a slight U-mineralisation represented by U-Ti oxides and uraninite (Grecula et al., 1995). The unstudied uranium-bearing *leucoxenes* exclusively represent U^{4+} minerals in the Šafárka occurrence.

Supergene-affected bodies of copper sandstones are characterised by a wide range of secondary Cu minerals, in which a significant place belongs to the arsenates. Supergene uranium minerals at the site have been studied only marginally so far. Unidentified secondary U minerals are already mentioned in the works of Ondrejkovič et al. (1964) and Drnzík (1965). Uranyl arsenates of Cu – metazeunerite (metaautunite group) and zeunerite (autunite group) were identified by Števko (2014) in the Bartolomej mining field at Novoveská Huta (Vojtechova horizon).

The formation of certain species/associations of uranyl minerals is governed by specific rules, which reflect the composition of the primary mineralisation, the nature of the host and surrounding rocks, their tectonic reworking, climatic conditions etc. The evolution of supergene transformations of U^{4+} minerals and their classification were compiled in many works (e.g., Belova, 2000, Krivovichev & Plášil, 2013). The primary minerals of Cu sandstones at the Šafárka occurrence are represented by sulphide phases (pyrite, chalcopyrite, tetrahedrite, tennantite, etc.), the weathering of which forms acidic environmental conditions (release of H_2SO_4). The acidic environment (pH < 7) is characteristic for the formation of uranyl phosphates/arsenates of the autunite and metaautunite group (autunite, uranocircite, metazeunerite, metatorbernite and so on) – so-called "*uranium micas*", which confirms the occurrence of zeunerite and metazeunerite in the copper sandstones at Novoveská Huta (Števko, 2014). At the Šafárka locality, despite the expected "*uranium micas*", the only supergene uranyl mineral is the Ca silicate – uranophane-α, although uranyl silicates typically precipitate under alkaline to neutral conditions (Eh > 0.2, pH ≥ 7) in an environment rich in Si (e.g., Langmuir, 1978; Finch & Ewing, 1992; Krivovichev & Plášil, 2013; Plášil, 2018). Hence, the formation of abundant uranophane-α in the studied locality documents the increase in the pH of the environment during weathering of sandstones and the formation of supergene minerals and can be explained as follows.

At a certain level of erosion cut, the bodies of copper sandstones came within the impact of supergene transformations, although under reducing conditions (low *f*O). Sulphides were degraded by supergene processes (reduction conditions), sulphuric acid was released from them (formation of the acidic environment), and also metal elements (Fe, Pb, Cu, Hg) and As. Sulphuric acid also reacted with rock-forming/accessory minerals of sandstone and U-Ti oxides (U-bearing *leucoxene*), releasing elements such as U, Ca, Ba, P, and Si into the solutions. At this stage, the cementation sulphides chalcocite and yarrowite were

formed, into which part of the released sulphur was bound. During the further progress of erosive cut, the sandstone bodies got to a shallower level – within reach of the oxidizing environment (high *f*O). At that time, the remaining S bound to the relatively insoluble sulphates – baryte and anglesite. Their formation gave rise to an increase in the pH of the environment (from acid to the slightly basic), which allowed the precipitation of uranophane and malachite. The mentioned mechanism also explains the presence of cementation and oxidation minerals next to each other in the studied samples. A similar neutralisation of the acidic environment at the occurrences of uranium mineralisation in the Western Carpathians, documented by the uranophane-α formation, was found at the Kravany deposit (Ferenc et al., 2003; Hoppanová, 2020) and the Východná-Nižný Chmelienec occurrence (Hoppanová et al., 2021).

Acknowledgements: This work was supported by the Slovak Research and Development Agency under the contract APVV-19-0065, as well as the Ministry of Education, Slovak Republic VEGA-1/0563/22 project. Authors thank to critics I. Rojkovič and J. Plášil for detailed reviews and improvement of the manuscript.

References

Abriatis P.K., Pattrick, R.A.D. & Vaughan D.J., 2004: Variations in the compositional, textural and electrical properties of natural pyrite: a review. *International Journal of Mineral Processing*, 74, 41–59.

Andráš P., Caňo F. & Stankovič J. 1998: Manifestations of Ni mineralisation at the Pezinok deposit. *Mineralia Slovaca*, 30, 309–310. [in Slovak]

Antaš J., 1963: Melafýry Vikartovského chrbta, ich petrografia a význam ako surovín. [Melaphyres of the Vikartovský chrbát Mts., their petrology and significance like raw materials]. Diploma thesis, Comenius University, Bratislava, 121 p. [in Slovak]

Bayliss P., 1989: Crystal chemistry and crystallography of some minerals within the pyrite group. *American Mineralogist*, 74, 1168–1176.

Belova L.N., 2000: Formation conditions of oxidation zones of uranium deposits and uranium mineral accumulations in the gipergenesis zone. *Geology of Ore Deposits*, 42, 103–110.

Bernard J.H., Rost R., Bernardová E., Breiter K., Kašpar P., Lang M., Melka K., Novák F., Rost J., Řídkošil T., Slivka D., Ulrych J. & Vrána S., 1992: Encyklopedický přehled minerálů. [Encyclopaedic overview of minerals]. Academia, Praha, 701 p. [in Czech]

Bhattacharyya S., Pal T., Sanyal S., Hazarika S. & Roy R., 2016: Control of crystal morphology on sector zoning in nickelian pyrite – a case study from wormhole tube, West Bengal, India. *In:* Online proceedings from 35th International Geological Congress, Cape Town, South Africa: https://www.americangeosciences.org/information/igc, n. p.

Bowles J.F.W., Howie R.A., Vaughan D.J. & Zussman J., 2001: Rock-forming minerals, Vol. 5A. Non-silicates – oxides, hydroxides and sulphides, 2nd edition. The Geological Society, London, 920 p.

Clark L.A. & Kullerud G., 1963: The sulphur-rich portion of the Fe-Ni-S system. *Economic Geology*, 58, 853–885.

Deditius A.P., Utsunomiya S., Renock D., Ewing R.C., Ramana C.V., Becker U. & Kesler S.E., 2008: A proposed new type of arsenian pyrite: Composition, nanostructure and geological significance. *Geochimica et Cosmochimica Acta*, 72, 2919–2933.

Deditius A.P., Utsunomiya S., Ewing R.C. & Kesler S.E., 2009: Nanoscale „liquid" inclusions of As-Fe-S in arsenian pyrite. *American Mineralogist*, 94, 391–394.

Drnzík E., 1965: Über ein besonderes erzvorkommen im Perm des nördlichen teiles der Gemeriden. *Geologické práce, Zprávy*, 35, 23–32. [in Slovak with German summary]

Drnzík E., 1969: Ore mineralization of copper bearing Permian snadstones type of melaphyre series on the North-eastern slopes of the Nízke Tatry Mts. *Mineralia Slovaca*, 1, 7–38. [in Slovak with English summary]

El Baz F. & Amstutz G.C., 1963: A statistical study of bravoite zoning. *Mineralogical Society of America, Special Paper*, 1, 190–197.

Evans A.M., 1993: Ore geology and industrial minerals. An introduction. Blackwell Science, Massachusetts, 389 p.

Faryad S.W., 1991[a]: Metamorphism of the Early Paleozoic salic to intermediate volcanic rocks. *Mineralia Slovaca*, 23, 325–332. [in Slovak with English summary]

Faryad S.W., 1991[b]: Metamorphism of the Early Paleozoic sedimentary rocks in Gemericum. *Mineralia Slovaca*, 23, 315–324. [in Slovak with English summary]

Ferenc Š., Rojkovič I & Maťo Ľ., 2003: Uranyl minerals of Western Carpathians. *In:* Zimák J. (Ed.) Proceedings of conference Mineralogie Českého masívu a Západných Karpát (Olomouc a Horní Údolí). Palacký University, Olomouc, pp. 17–23. [in Slovak with English abstract]

Finch R.J. & Ewing R.C., 1992: The corossion of uraninite under oxidizing conditions. *Journal of Nuclear Materials*, 190, 133–156.

Fleet M.E. & Mumin A.H., 1997: Gold bearing arsenian pyrite and marcasite and arsenopyrite from Carlin Trend gold deposit and laboratory synthesis. *American Mineralogist*, 82, 182–193.

Grecula P., Abonyi A., Abonyiová M., Antaš J., Bartalský B., Bartalský J., Dianiška I., Drnzík E., Ďuďa R., Gargulák M., Gazdačko Ľ., Hudáček J., Kobulský J., Lörincz L., Macko J., Návesňák D., Németh Z., Novotný L., Radvanec M., Rojkovič I., Rozložník L., Rozložník O., Varček C. & Zlocha J., 1995: Ložiská nerastných surovín Slovenského Rudohoria, zväzok 1 [Mineral deposits of the Slovak Ore Mountains Vol. 1]. Mineralia Slovaca, Košice, 829 p. [bilingual Slovak and English]

Hillebrand W. F., 1907: The Vanadium sulphide, patronite and its mineral associates from Minasragra, Peru. *American Journal of Science*, 24, 141–151.

Hoppanová E., 2020: Supergénne alterácie stratiformnej U-Cu mineralizácie v mladšom paleozoiku hronika Kozích chrbtov a Nízkych Tatier. [Supergene alterations of stratiform U-Cu mineralisation in the Late Paleozoic of Hronicum Unit in the Kozie Chrbty and Nízke Tatry Mts.]. Diploma thesis, Matej Bel University, Banská Bystrica, 88 p. [in Slovak]

Hoppanová E., Ferenc Š., Kopáčik R., Budzák Š. & Mikuš T., 2021: Supergene minerals from the U-Cu ore occurrence Východná-Nižný Chmelienec, the Nízke Tatry Mts. (Hronic Unit, Slovakia). *Bulletin Mineralogie Petrologie*, 29, 77–89. [in Slovak with English abstract]

Hók J., Pelech O., Teťák F., Németh Z. & Nagy A., 2019: Outline of the geology of Slovakia (W. Carpathians). *Mineralia Slovaca*, 51, 31–60.

Ivanička J., Snopko L., Snopková P. & Vozárová A., 1989: Gelnica Group – Lower Unit of Spišsko-gemerské Rudohorie Mts. (West Carpathians), Early Paleozoic. *Geologický Zborník Geologica Carpathica*, 40, 483–501.

Karup-Møller S. & Makovicky E., 1995: The phase system Fe-Ni-S at 725 °C. *Neues Jahrbuch für Mineralogie Monatshefte*, 1, 1–10.

Klemm D.D., 1965: Synthesen und alasysen in den dreickdiagrammen Fe-AsS-CoAsS-NiAsS und FeS_2-CoS_2-NiS_2. *Neues Jahrbuch für Mineralogie Abhandlungen*, 103, 205–255.

Kostov I. & Mincheva-Stefanova J., 1984: Sulfidnie mineraly, kristallochimija, paragenezis, sistematika. [Sulphide minerals, crystallochemy, paragenesis, systematics]. Mir, Moscow, 279 p. [in Russian]

Krivovichev S.V. & Plášil J., 2013: Mineralogy and crystallography of uranium. *In:* Burns P.C. & Sigmon G.E. (Eds.) Uranium: From cradle to grace, (Short Course 43). Mineral Assoc of Canada, Winnipeg, pp 15–119.

Langmuir D., 1978: Uranium solution-mineral equilibria at low temperatures with applications to sedimentary ore deposits. *Geochimica et Cosmochimica Acta*, 42, 547–569.

Laznicka P., 2006: Giant metallic deposits. Future sources of industrial metals. Springer-Verlag, Germany, 732 p.

Maheľ M. & Vozár J., 1971: Contribution to cognition of Permian and Triassic in the North-gemeric syncline. *Geologické Práce Správy,* 56, 47–66. [in Slovak with English summary]

Majzlan J., Drahota P. & Filippi M., 2014: Parageneses and crystal chemistry of arsenic minerals. *In:* Bowell R., Alpers Ch., Jamieson H., Nordstrom K. D. & Majzlan J. (Eds.): Reviews in mineralogy & geochemistry, Vol. 79. Arsenic – environmental geochemistry, mineralogy and microbiology. Mineralogical Society of America, Chantilly, Virginia, pp. 17–184.

Matula I., 1969: Contribution to the geochemistry of the Fichtenhübel pyrite (Spiš-Gemer Rudohorie Mts.). *Geologické Práce Správy*, 48, 81–90. [in Slovak with English summary] mindat.org/min-759.html, visited 20. 12. 2021.

Mello J., Ivanička J., Grecula P, Janočko J., Jacko S sr., Elečko M., Pristaš J., Vass D., Polák M., Vozár J., Vozárová A., Hraško Ľ., Kováčik M., Bezák V., Biely A., Németh A., Kobulský J., Gazdačko Ľ., Madarás J. & Olšavský M., 2008: General Geological map of the Slovak Republic, map sheet 37 – Košice. State Geological Institute of D. Štúr, Bratislava.

Németh Z., 2002: Variscan suture zone in Gemericum: Contribution to reconstruction of geodynamic evolution and metalogenetic events of Inner Western Carpathians. *Slovak Geological Magazine*, 8, 3–4, 247–257.

Novotný L. & Mihál' F., 1987: New lithostrathigraphical units in the Krompachy Group (eastern Slovakia). *Mineralia Slovaca*, 19, 97–113. [in Slovak with English summary]

Ondrejkovič K., Macko J., Kotras J, Drnzíková Ľ., Mandáková K. & Kroupa L., 1964: Záverečná správa a výpočet zásob Bindt-Novoveská Huta, Cu pieskovce. [Final report and resources calculation Bindt-Novoveská Huta, copper sandstones]. Unpublished Report, State Geological Institute of Dionýz Štúr archive, Bratislava, 271 p. [in Slovak]

Plášil J., 2018: Structural complexity of uranophane and uranophane-β: implications for their formation and occurence. *European Journal of Mineralogy*, 30, 253–257.

Polák Ľ., Ferenc Š. & Olšavský M., 2015: Výskyt uránovej mineralizácie v Selciach pri Banskej Bystrici [Occurrence of uranium mineralisation at Selce near Banská Bystrica]. *In:* Ondrejka M. (Ed.): Mineralogical-petrological conference Petros 2015. Comenius University, Bratislava, pp. 28–31. [in Slovak]

Polák Ľ., Ferenc Š., Mikuš T. & Sejkora J., 2017: New data on uranyl minerals from Selce occurrence at Banská Bystrica (North Veporicum Unit, Slovak Republic). *Bulletin Mineralogie Petrologie*, 25, 162–169. [in Slovak with English abstract]

Putiš M., Sergeev S., Ondrejka M., Larionov A., Siman P., Spišiak J., Uher P. & Paderin I., 2008: Cambrian-Ordovician metaigneous rocks associated with Cadomian fragments in the West-Carpathian basement dated by SHRIMP on zircons: a record the Gondwana active margin setting. *Geologica Carpathica*, 59, 3–18.

Quian G.J., Brugger J., Testemale D., Skinner W. & Pring A., 2013: Formation of As(II)-pyrite during experimental replacement of magnetite under hydrothermal conditions. *Geochimica et Cosmochimica Acta*, 100, 1–10.

Radvanec M., Németh Z., Kráľ J. & Pramuka S., 2017: Variscan dismembered metaophiolite suite fragments of Paleo-Tethys in Gemeric Unit, Western Carpathians. *Mineralia Slovaca*, 49, 1–48.

Radvanec M. & Németh Z. 2018: Variscan epidote-eclogite blueschists and pumpellyite-actinolite facies Cpx/Sr rich epidote metagabro blocks exhumed in Carboniferous with Permian amphibolite facies overprint (Gemeric Unit, Western Carpathians). *Mineralia Slovaca*, 50, 55–99.

Reich M. & Becker U., 2006: Forst principles calculations of the thermodynamic mixing properties of arsenic incorporation into pyrite and marcasite. *Chemical Geology*, 225, 278–290.

Riley J.F., 1965: An intermediate member of the binary system FeS_2 (pyrite)-CoS_2 (cattierite). *American Mineralogist*, 50, 1083–1086.

Riley J.F., 1968: The cobaltiferous pyrite series. *American Mineralogist*, 53, 293–295.

Řídkošil T., 1977: Některé druhotné minerály ze Španí Doliny a Novoveské Huty. [Some secondary minerals from Špania Dolina and Novoveská Huta]. Diploma thesis, Charles University, Praha, 101 p. [in Czech]

Řídkošil T., 1978: Novoveská Huta – nová lokalita vzácných druhotných nerostů mědi. [Novoveská Huta – new locality of rare secondary copper minerals]. Časopis pro mineralogii a geologii, 23, 214. [in Czech]

Řídkošil T., 1981: Clinoclase from Novoveská Huta, Slovakia. *Acta Universitatis Carolinae, Geologie*, 1, 45–52.

Řídkošil T., 2007: Novoveská Huta – lokalita vzácnych sekundárních minerálů mědi. [Novoveská Huta – locality of the rare secondary copper minerals]. *Minerál*, 15, 445–447. [in Czech]

Rojkovič I., 1985: Ore mineralization of ultramafic bodies of the Western Carpathians. Veda publishing house of SAS, Bratislava, 112 p. [in Slovak with English summary]

Rojkovič I., 1997: Uranium mineralization in Slovakia. Acta Geologica Slovaca - Monographic serie, Comenius University, Bratislava, 117 p.

Rojkovič I., 1998: Stratiform U-Cu mineralization in the Permian rocks of the Nízke Tatry Mts. *Mineralia Slovaca*, 30, 66–71. [in Slovak with English summary]

Rojkovič I., 2003: Copper sandstones of Gemeric Unit, Western Carpathians. *In:* Zimák J. (Ed.): Mineralogie Českého masivu a Západních Karpat. Sborník referátů ze semináře. Palacký University, Olomouc, pp. 42–44. [in Slovak with English abstract]

Rosso K.M. & Vaughan D.J., 2006: Sulfide mineral surfaces. *In:* Vaughan D.J. (Ed.): Reviews in mineralogy & geochemistry, Vol. 79. Sulfide mineralogy nad geochemistry. Mineralogical Society of America, Chantilly, Virginia, pp. 505–556.

Snopko L. & Ivanička J., 1978: Considerations on the paleogeography in the Lower Paleozoic of Spišsko-gemerské Rudohorie Mts. *In:* Vozár J. (Ed.) Paleogeographical evolution of the Western Carpathians. Geological Institution of D. Štúr, Bratislava, pp. 269–280. [in Slovak with English abstract]

Števko M., 2014: Mineralogická charakteristika supergénnych arzeničnanov medi z lokalít Novoveská Huta, Poniky a Špania Dolina. [Mineralogical characteristic of supergene Cu arsenates from the Novoveská Huta, Poniky and Špania Dolina localities]. PhD thesis, Comenius University, Bratislava, 134 p. [in Slovak]

Števko M., Sejkora J. & Malíková R., 2018: New data on supergene minerals from the Banská Štiavnica deposit (Slovak Republic). *Bulletin Mineralogie Petrologie*, 26, 90–101. [in Slovak with English abstract].

Varček C., 1971: Identification of some accessory nickel minerals occuring on the siderite deposits of the Spiš-Gemer Rudohorie Mts. by electron-probe microanalyser. *Mineralia Slovaca*, 3, 231–236. [in Slovak with English abstract]

Varček C., 1977: Niektoré zriedkavejšie typy mineralizácie v Spišsko-gemerskom rudohorí. [Some rare types of mineralisation in the Spišsko-gemerské rudohorie Mts.]. *In:* Háber M. (Ed.) Ložiskotvorné procesy Západných Karpát – zborník z konferencie. [Deposit forming processes in the Western Carpathians, conference proceedings]. Comenius University, Bratislava, pp. 93–99. [in Slovak]

Vaughan D.J., 1969: Zonal variation in bravoite. *American Mineralogist*, 54, 1075–1083.

Vozárová A., 1993: Variscan metamorphism and crustal evolution of the Gemericum. *Západné Karpaty Sér Min Petr Metalog Geoch*, 16, 55–117. [in Slovak with English abstract]

Vozárová A., 1996: Tectono-sedimentary Evolution of Late Paleozoic Basins based on interpretation of litostratigraphic data (Western Carpathians; Slovakia). *Slovak Geological Magazine*, 3–4, 251–271.

Vozárová A., Konečný, P., Šarinová K. & Vozár J., 2014: Ordovician and Cretaceous tectonothermal history of the Southern Gemericum Unit from microprobe monazite geochronology (Western Carpathians, Slovakia). *International Journal of Earth Sciences*, 103, 4, 1005–1022.

Watson E.B., 1996: Surface enrichment and trace element uptake during crystal growth. *Geochimica et Cosmochimica Acta*, 60, 5013–5020.

webmineral.com/data/Bravoite.shtml#.Ye6DQPg1WvQ, visited 20. 12. 2021.

Wolf K.H. (Ed.), 1976: Handbook of strata bound and stratiform ore deposits. Vol. 6, Cu, Zn, Pb and Ag deposits. Elsevier Scientific Publishing Company, Netherlands, 584 p.

Zhang H., Qioan G., Cai Y., Gibson Ch. & Pring A., 2022: The crystal chemistry of arsenian pyrites: A Raman spectroscopic study. *American Mineralogist*, 107, 2, 274–281.